Composite Structures 94 (2012) 1626–1633

Contents lists available at SciVerse ScienceDirect

Composite Structures

journal homepage: www.elsevier.com/locate/compstruct

Optimal design of variable fiber spacing composites for morphing aircraft skins

Senthil Murugan [a,*], Erick I. Saavedra Flores [a,b], Sondipon Adhikari [a], M.I. Friswell [a]

[a] School of Engineering, Swansea University, Singleton Park, Swansea SA2 8PP, UK
[b] Departamento de Ingeniería en Obras Civiles, Universidad de Santiago de Chile, Av. Ecuador 3659, Santiago, Chile

ARTICLE INFO

Article history:
Available online 11 January 2012

Keywords:
Aircraft skins
Elastomer materials
Variable fiber composites
Optimization

ABSTRACT

Morphing aircraft concepts aim to enhance the aircraft performance over multiple missions by designing time variant wing configurations. The morphing concepts require wing skins that are flexible enough to allow large in-plane stretching and high bending stiffness to resist the aerodynamic loads. In this study, an optimization problem is formed to enhance the in-plane flexibility and bending stiffness of wing skins made of composite laminate. Initially, the optimal fiber and elastomer materials for highly flexible fiber reinforced elastomer laminates are studied using materials available in the literature. The minor Poisson's ratio of the laminate is almost zero for all the fiber and elastomer combinations. In the next stage, the effects of boundary conditions and aspect ratio on the out-of-plane deflection of the laminate are studied. Finally, an optimization is performed to minimize the in-plane stiffness and maximize the bending stiffness by spatially varying the volume fraction of fibers of a laminate. The optimization results show that the in-plane flexibility and bending stiffness of the laminate with a variable fiber distribution is 30–40% higher than for the uniform fiber distribution.

1. Introduction

In recent years, considerable research has focussed on designing aircraft wings which can reconfigure their initial wing shape to the optimal shape of a specific flight regime. The aircraft wings capable of such a reconfiguration in shape in flight, are termed morphing wings [1]. The possible morphing wing abilities include variable sweep, dihedral position, chamber change, wing chord change and wing span change. One of the key challenges in developing a successful morphing wing is the development of morphing skin that is a continuous layer of material that would stretch over the morphing structure to form a smooth aerodynamic surface. Most research on morphing skin technology can be broadly classified under three major areas [2]: Compliant structures, shape memory polymers (SMPs) and anisotropic elastomeric skins. A good review on the compliant structures and shape memory polymers for morphing skin applications can be found in Ref. [1].

Elastomer skins have high strain capability, lower degree of risk due to their passive operation, elastic recovery with nominal strain values and a smooth aerodynamic surface characteristics which make them a desirable candidate for morphing skins [3,4]. These materials include thermoplastic polyurethanes, copolyester elastomer, and woven materials made from elastane yarns. A very few studies have investigated the elastomeric skins tailored specifically for span-morphing applications with a suitable supporting substructure to withstand aerodynamic loads.

Peel et al. [3] developed a wing skin, actuator, and actuator attachment for a simple morphing wing. Upper and lower wing skins were fabricated with carbon fiber/polyurethane elastomer laminates. An elastic camber down of 25° at the nose and 20° at the tail were achieved. Bubert [5] studied the properties of various silicone elastomers for the morphing skins. The most promising silicone elastomer was Rhodorsils V-330 CA-45 which had the right combination of low viscosity and long work time to enable easy and effective fiber-reinforced elastomer composite manufacture, and demonstrated high maximum elongation and tear strength.

Kikuta [6] investigated the mechanical properties of elastomers that could be used as a skin for morphing wings. The materials tested were thermoplastic polyurethanes, copolyester elastomer, woven materials and shape memory polymers. The materials which strained well and required less force, could not sustain high pressure loads. The materials that did not strain well and required more actuation force were able to handle a larger sustained pressure load. Finally, the study suggested that Tecoflex 80A was the best elastomer for morphing skin applications. Murray et al. [4] developed mathematical models of Flexible Matrix Composite (FMC) skin panel and validated against experiments. FMC was constructed using glass fibers and Dragon Skin Shore 10A elastomer matrix. This study compared the FMC skin to a matrix-only skin and illustrated the importance of the fibers stiffness in tolerating pretension and limiting the out-of-plane deformation under load. Also, the panel size

* Corresponding author. Tel.: +44 (0)1792 602969; fax: +44 (0)1792 295676.
E-mail address: s.m.masanam@swansea.ac.uk (S. Murugan).

0263-8223/$ - see front matter © 2012 Elsevier Ltd. All rights reserved.
doi:10.1016/j.compstruct.2011.12.023

and lengths in the non-morphing direction of skins were found to have considerable influence on the out-of-plane deformation. In general, fiber and matrix modulus has a limited effect on out-of-plane deformation of flexskin panels.

The main focus of the studies discussed above were the selection of proper materials for the skin. The design and optimization of laminates for the morphing skin application is another key area of research. With the conflicting objectives of low in-plane stiffness, high out-of-plane bending stiffness and zero Poisson's ratio, the nature of design variables selected for optimization has to be different from that of conventional composite structures. For example, conventional composite laminates are made of plies with the fibers being straight, parallel and uniformly spaced. However, for a morphing skin application, the curvilinear fiber-format, termed as variable stiffness laminates or variable fiber spacing composites, can be beneficial as it can decouple the conflicting requirements of morphing skins [7,8].

Martin and Leissa [8] investigated the plane stress problem of a composite laminate with spatially varying volume fraction of fibers. The fiber redistribution increased the buckling load by as much as 38%. Benatta et al. [9] demonstrated the improvements in the structural properties of beams by creating functionally graded materials (FGM) in the form of a symmetric composite whose fiber volume fraction varies through the thickness. Kuo and Shiau [10] have shown that the more fibers distributed in the central portion of the plate can efficiently increase the buckling load and natural frequencies. Kuo [11] has shown that the supersonic flutter boundary can be increased or decreased due to variable fiber spacing of composite plates. The above studies have focussed on the vibration, buckling and flutter of composite plates. However, the variable volume fraction of fibers can also be used to achieve some of the design requirements of morphing skins, and is the aim of this study.

In this study, two essential features of morphing skins are investigated. In the first part, the optimal combination of fiber and elastomer matrix available for morphing wing skins are investigated with a simple micromechanial model of the laminate. The second part involves an optimization process to find the optimal distribution of volume fraction of fibers in a laminate to minimize the in-plane stiffness and maximize the out-of-plane stiffness, simultaneously. In addition, the previous studies considered similar distribution of variable fibers for all the plies in a laminate [8,10,11]. However, in this study, the variable fiber distribution of each ply of the laminate is considered as independent.

2. Elastomer materials

The wing span extension type morphing mechanisms require the in-plane stretching of wing skins to be more than 25% strain without failure. Conventional fiber reinforced epoxy laminates have tensile failure strains in the range of 1–2% in the fiber direction and transverse tensile failure strains of around 0.5% [12]. The elastomers are one of the few materials that can undergo strains more than 25% without failure. This section explore the mechanical properties of fiber reinforced elastomer (FRE) lamina with various elastomers and fibers available in the literature. The preliminary results can help to find the optimal fiber and elastomer combination and highlight issues related to the design of FRE laminates for morphing skins.

The fibers and elastomer material properties collected from the literature are given in Tables 1 and 2. The elastomer properties are collected from Refs. [3,6]. Most of the elastomers exhibit linear stress–strain behavior for strains up to 25% and exhibit non-linear properties after that [6]. The properties of elastomers in the linear strain range are given in Table 2. The lamina is modeled with the fibers perpendicular to the in-plane stretching or morphing direction as shown in Fig. 1. The lamina properties are evaluated with a micro-mechanical model based on the rule of mixtures for all the combinations of fibers and elastomers given in Tables 1 and 2 [13]. The longitudinal Young's modulus, lateral modulus, major and minor Poisson's ratio of the FRE lamina are shown in Figs. 2 and 3.

Table 1
Fibers properties.

Material	E_1 (GPa)	E_2 (GPa)	ν_{12}	G_{12} (GPa)
Kevlar (29)	61	4.2	0.35	2.9
Glass	71	71	0.22	30
Kevlar (49)	154	4.2	0.35	2.9
Graphite (AS)	224	14	0.2	14
Saffil	300	300	0.2	126
Graphite (HMS)	385	6.3	0.2	7.7
Al_2O_3	385	385	0.3	154
SiC	406	406	0.2	169
Boron	420	420	0.2	170

Table 2
Matrix properties.

Material	E_1(MPa)	ν_{12}	G_{12} (MPa)	@ Strain (%)
Silicone rubber	0.916	0.50	0.3053	–
Tecoflex 80A	1.07	0.75	0.3057	21.3
RP6410 urethane	1.65	0.50	0.549	–
RP6442 urethane	6.095	0.50	2.034	–
Tecoflex 100A	16.6	0.50	5.5333	20.8
Arnitel 640A	23.5	0.33	8.8346	23.7
Riteflex 640A	35.8	0.60	11.1875	22.2
RP6444 urethane	182	0.50	60.6	–
Typical epoxy	2096	0.30	806	3–4 (failure)

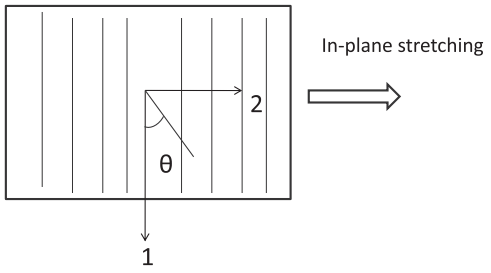

Fig. 1. Fiber reinforced lamina.

The longitudinal Young's modulus show a variation of 20–220 GPa for the various fiber and elastomer combinations. The out-of-plane bending strength of the FRE skin depends on the longitudinal Young's modulus. The lateral Young's modulus, a parameter corresponding to the in-plane stretching of the FRE skins, varies from 10 to 400 MPa, which is of the order of 10^3 less than the longitudinal modulus. The shear modulus also varies in a similar way to the lateral Young's modulus. The major Poisson's ratio of the FRE lamina varies from 0.2 to 0.55 as shown in Fig. 3a. Peel has shown that the in-plane Poisson's ratios of FRE can reach higher than 32 and less than −60 [14]. However, for a wing span extension type morphing mechanism, the major Poisson's ratio in consistent with Fig. 1 does not play a major role whereas the minor Poisson's ratio has to be small. The minor Poisson's ratio of the FRE lamina shown in Fig. 3b is of the order of 10^{-3} for all the fiber and elastomer combinations. This is because the minor Poisson's ratio depends on the ratio of transverse to longitudinal modulus, as given in Eq. (1), which is of the order of 10^{-3} for the FRE composites considered.

$$\upsilon_{21} = \frac{E_2}{E_1}\upsilon_{12} \tag{1}$$

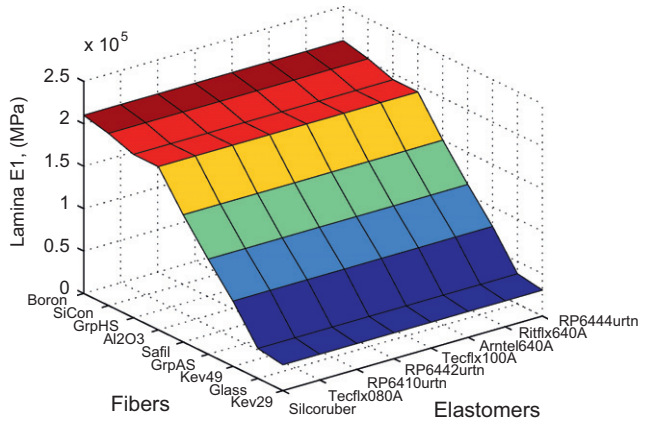

(a) Longitudinal Young's modulus

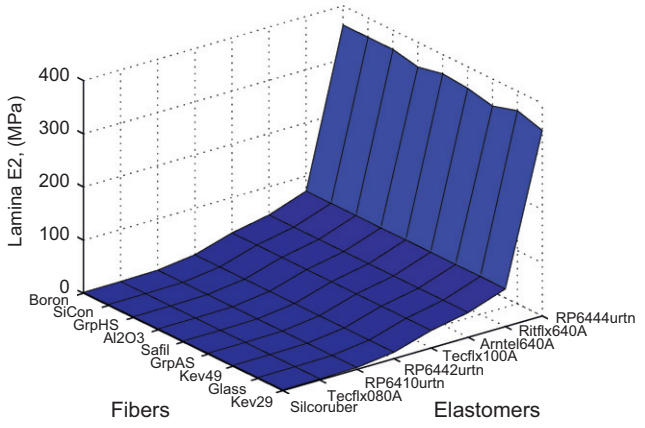

(b) Lateral Young's modulus

Fig. 2. Modulus properties of lamina for various fiber and elastomer materials for strains less than 25%.

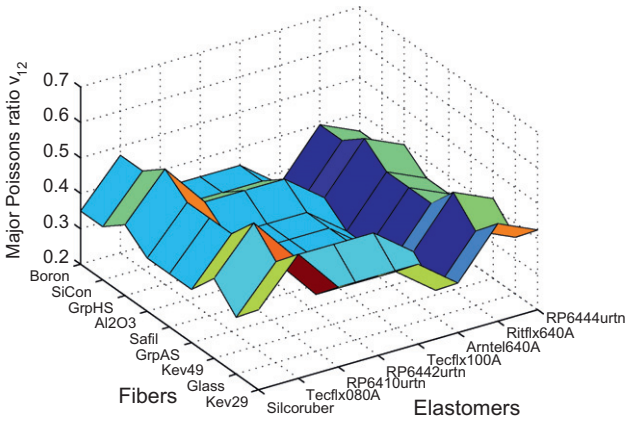

(a) Major Poisson's ratio

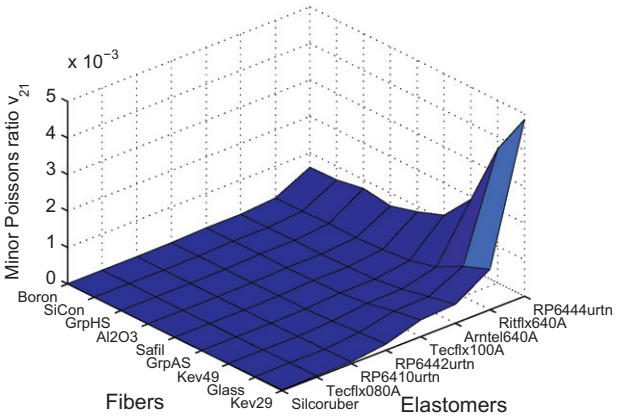

(b) Minor Poisson's ratio

Fig. 3. Poisson's ratio of laminae for various fiber and elastomer materials for strains less than 25%.

These preliminary results show that the fiber and elastomer combinations considered in this study have considerable variations in the longitudinal Young's modulus and major Poisson's ratio property. Meanwhile, all the fiber and elastomer combinations satisfy the lateral Young's modulus and minor Poisson's ratio requirements desirable for the morphing skins. However, the FRE lamina properties can vary with the non-linear stress–strain behavior of the elastomer for strains more than 25% and the elastic recovery, the fiber-elastomer bonding and thermal properties can play a major role in the selection of a elastomer for the morphing skins.

3. Optimization problem

In this section, an optimization is performed to find the optimal fiber distributions of composite plates representative of morphing skins. The objective is to maximize the ratio of in-plane stretching to the out-of-deflection of a laminate by varying the fiber volume distribution. The optimization is performed for two cases. In the first case, the maximum out-of-plane deflection for a given uniform pressure loading is minimized. In the second case, the ratio of in-plane displacement to the maximum out-of-plane displacement is maximized. That is the laminate is optimized to be flexible along the in-plane direction and stiffened enough to minimize the out-of-plane deflection due to uniform pressure loading, simultaneously.

The morphing wing skin panels can be modeled with different aspect ratios (ARs) and with different possible boundary conditions. Therefore, before performing the optimization, the effects of aspect ratio on the out-of-plane deflection of skin panels modeled as plates are studied in Section 3.1. Similarly, the mechanical properties of the lamina for various volume fractions of fibers is calculated with a homogenization-based multi-scale constitutive model, which is discussed in Section 3.2.

3.1. Out-of-plane deflection

An aluminum plate and a composite plate with the same structural dimensions are considered to study the effect of aspect ratio on the out-of-plane deflections. The composite plate is made of graphite fibers and epoxy matrix given in Tables 1 and 2. Two possible boundary conditions representative of the morphing skin are considered. In the first case, the boundary conditions of the plate are simply supported at two sides and fixed at other two sides (SS–FF). In the second case, the boundary condition of the plate are fixed at all four sides (FF–FF). In the first case, the fibers of the composite plate are parallel to the fixed edges. This represents a morphing skin which is allowed to morph in the spanwise direction.

The maximum out-of-plane displacement Δ^{max} of the plate due to uniform pressure loading is evaluated with ANSYS for aspect ratios varying from 0.5 to 2.0 [15]. The percentage increase in Δ^{max} for different aspect ratios are compared to Δ^{max} at an aspect ratio of 1.0 and is shown in Figs. 4 and 5. The results show that the deflection of an isotropic plate increases almost 100% with an increase in the aspect ratio from 1 to 2 for the FF–FF boundary condition. Further, the increase in deflection converges around the aspect ratio of 2.0. However, for the orthotropic plate, the deflec-

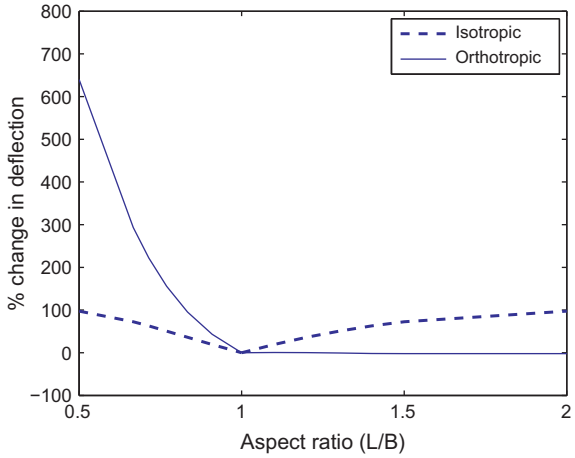

Fig. 4. Effects of aspect ratio on the out-of-plane displacement for a plate with FF–FF conditions.

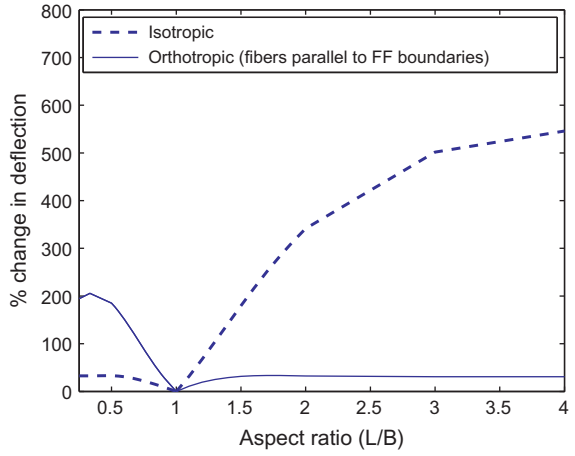

Fig. 5. Effects of aspect ratio on the out-of-plane displacement for a plate with SS–FF conditions.

tion remains constant with the increase in aspect ratio (L/B ratio), whereas it increases dramatically with the L/B ratio less than 1. For example, the deflection increases by 600% for the L/B ratio of 0.5 as shown in Fig. 4.

For the SS–FF boundary condition case, the deflection of the orthotropic plate increases to almost 30% when the aspect ratio reaches 1.5 and remains relatively constant after that, as shown

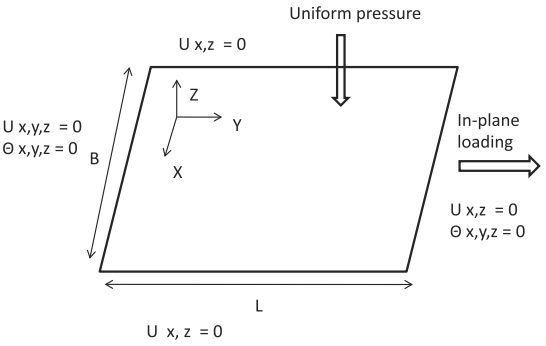

Fig. 7. Boundary conditions of laminate.

in Fig. 5. As the composite fibers are in the direction perpendicular to the simply supported boundary conditions, the change from a square plate to a rectangular plate has little effect on the composite plates for an L/B ratio greater than 1. However, when the aspect ratio is less than 1, the deflection of the composite plate increases dramatically compared to the isotropic plate. This is due to the fact that E_2, which is much less than E_1 for the composite plate, plays a major role in the out-of-plane bending for aspect ratios less than 1. Note, the thickness of the plate is kept constant for all aspect ratios. These results show that the optimal design of the plates can vary with the aspect ratio. Therefore, the optimization has to be performed for different aspect ratios. In the following sections, the optimization is performed to find the optimal distribution of composite fibers of the plate with the aspect ratios of 1.0, 1.3, 2.0 and 4.0.

3.2. Homogenization-based multi-scale constitutive model

The micro-mechanical model in this study used to calculate the lamina properties for varying volume fraction of fibers is discussed in the following. The main assumption in the homogenization-based multi-scale constitutive theory of heterogenous solids is that the macroscopic or homogenized strain tensor $\boldsymbol{\epsilon}$ at any arbitrary point $\boldsymbol{x}$ of the macroscopic continuum is the volume average of the microscopic strain tensor field $\boldsymbol{\varepsilon}_\mu$ defined over a local representative volume element (RVE). The RVE is such that its domain Ω_μ has a characteristic length much smaller than that of the macroscopic continuum and, at the same time, is sufficiently large to represent the mechanical behavior of the heterogeneous medium in the averaged sense.

At any instant t, the macroscopic or homogenized strain tensor $\boldsymbol{\varepsilon}$ at a point $\boldsymbol{x}$ can be expressed as

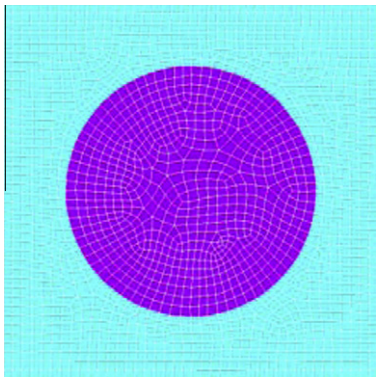

Fig. 6. Representative volume element (RVE).

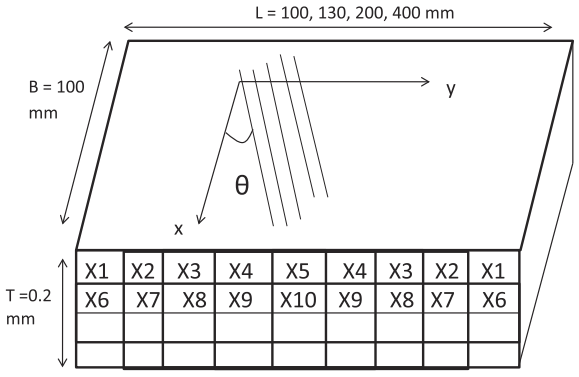

Fig. 8. Laminate with volume fraction of fibers as design variables.

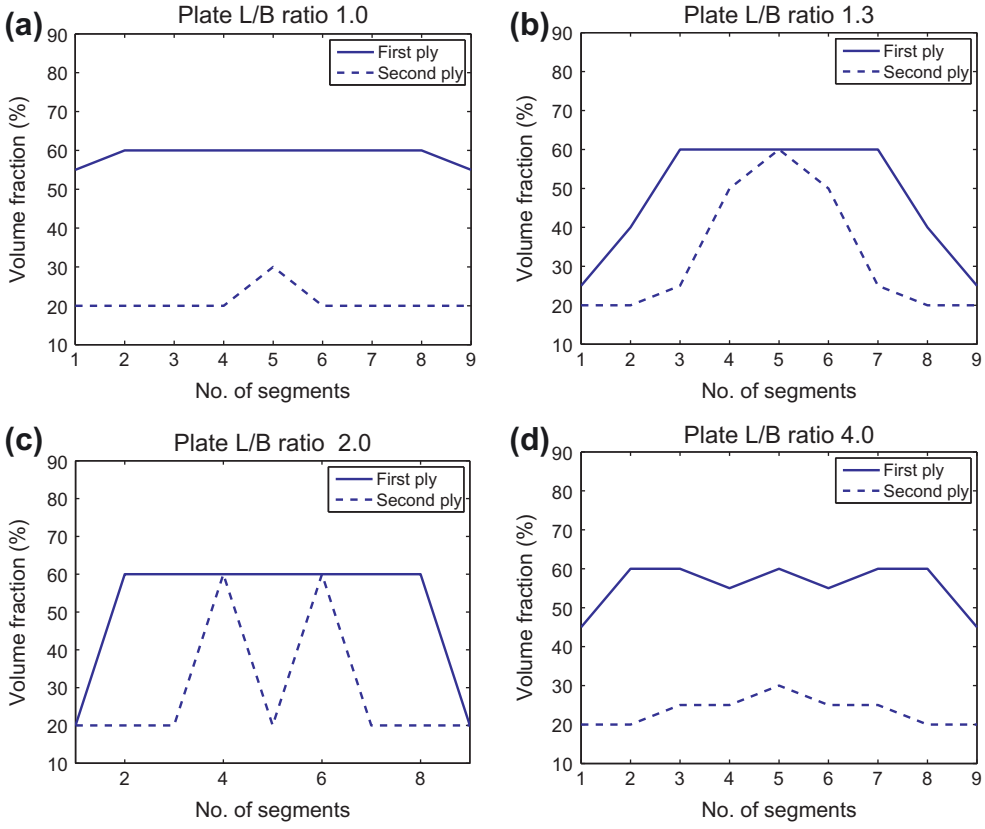

Fig. 9. Optimal distribution of volume fraction of fibers, case I.

Table 3
Maximum out-of-plane displacement for variable fiber distributions.

Plate L/B ratio	Δ_{40} ($/\Delta_{40}$)	$\Delta_{60/20}$ ($/\Delta_{40}$)	Optimal case I ($/\Delta_{40}$)
1.0	1.0	0.7361	0.7384
1.3	1.0	0.7319	0.7156
2.0	1.0	0.7320	0.7081
4.0	1.0	0.7323	0.7685

$$\boldsymbol{\varepsilon}(\boldsymbol{x},t) = \frac{1}{V_\mu}\int_{\Omega_\mu} \boldsymbol{\varepsilon}_\mu(\boldsymbol{y},t)\,dV \tag{2}$$

where V_μ is the volume of the RVE associated to point $\boldsymbol{x}$, $\boldsymbol{y}$ denotes the local RVE coordinates and $\boldsymbol{\varepsilon}_\mu = \nabla^s \boldsymbol{u}_\mu$, with ∇^s denoting the symmetric gradient operator and $\boldsymbol{u}_\mu$ the RVE (or microscopic) displacement field.

Further, it is possible to decompose the displacement field $\boldsymbol{u}_\mu$ as a sum of a linear displacement $\boldsymbol{\varepsilon}(\boldsymbol{x},t)\boldsymbol{y}$, which represents a homogeneous strain, and a displacement fluctuation field $\tilde{\boldsymbol{u}}_\mu$, i.e.,

$$\boldsymbol{u}_\mu(\boldsymbol{y},t) = \boldsymbol{\varepsilon}(\boldsymbol{x},t)\boldsymbol{y} + \tilde{\boldsymbol{u}}_\mu(\boldsymbol{y},t) \tag{3}$$

The displacement fluctuations field represents local variations about the linear displacement $\boldsymbol{\varepsilon}(\boldsymbol{x},t)\boldsymbol{y}$ and do not contribute to the macroscopic scale strain. The field $\tilde{\boldsymbol{u}}_\mu$ depends on the presence of heterogeneities within the RVE.

In general, the present multi-scale constitutive theory requires the prescription of kinematical constraints upon the selected RVE. In what follows, the choice of this set of kinematical constraints will coincide with the widely used *Periodic boundary displacement fluctuations* model. This is typically associated with the modeling of periodic media. The fundamental kinematical assumption in this class of constitutive models consists in prescribing identical displacement fluctuation vectors for each pair of opposite points $\{\boldsymbol{y}_+, \boldsymbol{y}_-\}$ on the RVE boundary $\partial\Omega_\mu$, such that:

$$\tilde{\boldsymbol{u}}_\mu(\boldsymbol{y}_+,t) = \tilde{\boldsymbol{u}}_\mu(\boldsymbol{y}_-,t) \quad \forall\ \{\boldsymbol{y}_+,\boldsymbol{y}_-\} \in \partial\Omega_\mu. \tag{4}$$

The adopted RVE in the present work is shown in Fig. 6. We consider a periodic linear elastic medium with a circular reinforcing fiber located in the center of the RVE, embedded in a softer matrix. The volume fraction of reinforcement considered here are: 20%, 30%, 40%, 50% and 60%. The finite element implementation of the homogenization scheme was carried out in ANSYS [15]. For further details about computer implementation of this type of models, we refer, for instance, to [16,17]. Three-dimensional solid structural elements (Solid45) were used in all the RVE finite element meshes. The lamina properties for volume fractions of fibers between 20% and 60% are calculated with the graphite fiber and epoxy matrix materials given in Tables 1 and 2.

3.3. Optimization formulation

In this section, the optimization is performed to find the optimal distribution of fibers with the conclusions drawn from the previous sections. The boundary conditions of a laminate representative of a morphing skin is shown in Fig. 7. The plate is divided into 9 sections along the length 'L', as shown in Fig. 8. The term aspect ratio or L/B ratio is interchangeable in the following discussions. A symmetric balanced laminate with four plies is considered in this study. The design variables X_1 to X_{10}, shown in Fig. 8, represent the volume fraction of fibers. The upper and lower limits of the volume fraction of fibers in a laminate depends on the fiber packing and failure modes [13,18]. The design variables are allowed to vary between 20% and 60% volume fraction of fibers with a 5% increment while the average volume fraction of the laminate is kept at 40%. That is

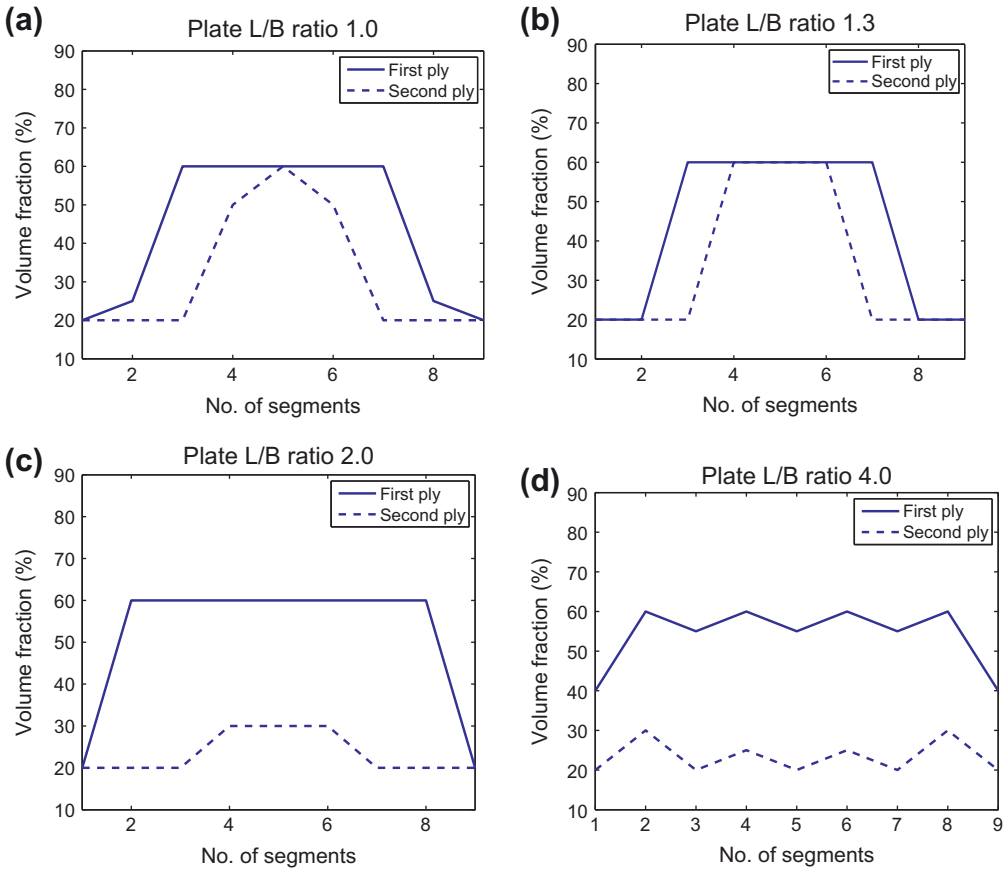

Fig. 10. Optimal distribution of volume fraction of fibers, case II.

Table 4
Flexibility ratio for variable fiber distributions.

Plate L/B ratio	$(FR)_{40}$	$(FR)_{60/20}$	Optimal case I	Optimal case II
1.0	9.1177	11.7807	11.8038	12.5530
1.3	10.0894	13.1089	14.2684	14.9080
2.0	15.4054	20.0147	21.6622	21.8947
4.0	30.9345	40.1732	39.5447	40.6432

Table 5
Percent increase in flexibility ratio for variable fiber distributions.

Plate L/B ratio	$(FR)_{60/20}$	Optimal case I	Optimal case II
1.0	29.21	29.46	37.68
1.3	29.93	41.42	47.76
2.0	29.92	40.61	42.12
4.0	29.87	27.83	31.38

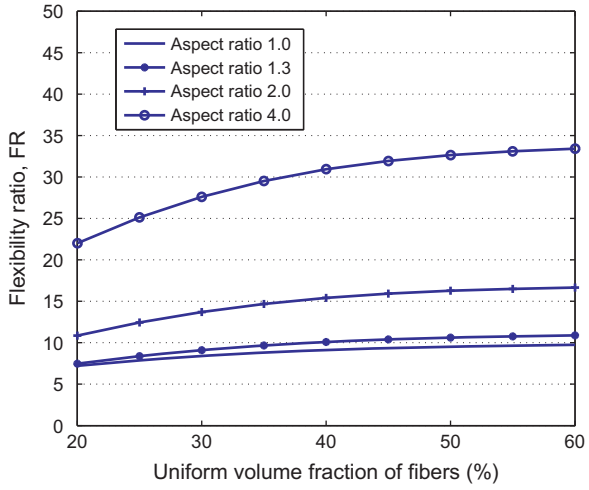

Fig. 11. Variation of flexibility ratio with the volume fraction of fibers of lamina.

the fibers of a plate with the uniform volume fraction of 40% is redistributed to improve its structural efficiency. A uniform pressure of 50 Pa is applied to the surface and a uniform in-plane loading of 1 N/mm is applied along the edge of the plate. The maximum out-of-plane displacement and in-plane displacement for the given loadings are calculated using ANSYS with shell99A elements.

The objective function to minimize the maximum out-of-plane displacement of the plate and constraints for the optimization case I can be written as

$$Minimize,\ \left[\frac{\Delta(X)^{max}}{\Delta_{40}^{max}}\right] \tag{5}$$

The constraint is

$$g(X) = \frac{\sum_{i=1}^{n}(X_i)}{n} = 40\% \tag{6}$$

where $\Delta(X)^{max}$ is the maximum out-of-plane displacement of plate and the X_i are the design variables, that is the volume fraction of fibers (%). The displacement Δ_{40}^{max} denotes the value corresponding to the plate with uniform fiber volume fraction of 40%. Thus the uniform fiber distribution with 40% volume fraction is considered as the baseline design.

Similarly, the objective function to minimize the maximum out-of-plane displacement of the plate and maximize the in-plane displacement for optimization case II can be written as

$$\text{Maximize}, \quad \left[w_1 \left(\frac{\delta(X)}{\delta_{40}} \right) + w_2 \left(\frac{\Delta_{40}^{max}}{\Delta(X)^{max}} \right) \right] \tag{7}$$

where $\delta(X)$ is the in-plane displacement of the plate, and w_1 and w_2 are the weights of the functions. Here, the two objective functions are combined to form a single aggregate objective function using the weighted linear sum of the objectives method. In this study, equal weights are assigned to both the objective functions, i.e., $w_1 = 0.5$ and $w_2 = 0.5$. The optimization case II has the same constraint as given in Eq. (6). The ply angle values are assigned to be zero while optimizing the fiber distribution. It is likely that the optimal ply angle values will be zero for the boundary conditions and objective function of this problem.

The optimization is performed with a real coded genetic algorithm (GA) coupled with the ANSYS for objective function evaluations [19]. The optimization was performed with a population size of 40 and 200 generations. The main issue, in terms of computational time, in this optimization study was the implementation of constraints given in Eq. (6). The constraint requires the average value each potential design, i.e., the average of volume fraction of the fibers, to be equal to 40%. However, the GA creates the new designs which may not satisfy the constraints, thereby increasing the number of generations to find the optimal solution.

3.3.1. Optimization case I

The optimization is performed for aspect ratios of 1.0, 1.3, 2.0 and 4.0. The results of the optimization case I are shown in Fig. 9 and Table 3. The optimal fiber distribution for the AR of 1.0 shows that the top ply has almost 60% volume fraction (VF) and the second ply has 20% VF. For the AR of 1.3, the optimal result shows a parabolic type distribution for both the ply layers with almost 30% VF at the edges and reaching 60% at the middle of the plate length, L. For the AR of 2.0, the optimal distribution of the top ply shows a parabolic type distribution whereas the second layer shows a dual peak type distribution. Similarly, for the AR of 4.0, the fiber volume distribution has multiple peaks for both of the ply layers.

The maximum out-of-plane deflections of optimal fiber distributions are compared with the maximum out-of-plane deflections of uniform fiber distributions and given in Table 3. In addition to the optimal case and uniform fiber distribution case, the fiber distribution of 60% VF at the top layer and 20% VF at the second layer, so that the average VF is 40%, is also given in Table 3. For easy comparison, all deflections are normalized with the deflections of the uniform fiber distribution (Δ_{40}). The results show that the optimal distributions corresponding to the AR 1.3 and 2.0 are better than the 60/20 VF case whereas for the AR of 1.0 and 4.0, the 60/20 VF case is slightly better than the optimal distributions. However, both the 60/20 VF case and optimization results show almost 20–30% reduction in the deflection compared to the uniform distribution of 40% VF. These results show that more fibers at the ply layers away from the neutral axis increase the bending strength of a laminate considerably.

3.3.2. Optimization case II

The optimization case II is performed with the objective function and constraints given in Eqs. (7) and (6), respectively. The results of the optimization are shown in Fig. 10. A flexibility ratio (FR) is defined as the percentage of in-plane displacement to the maximum out-of-plane displacement of the plate, i.e., FR = $(\delta/\Delta) * 100$. This flexibility ratio, in terms of stiffness, measures the in-plane flexibility for an unit out-of-plane bending stiffness. The FR ratio is given for the optimization results of case I and II, the 60/20 VF case and the uniform fiber distribution case in Table 4. Similarly, the percentage increase in the FR of optimal results and the 60/20 VF case compared to that of uniform fiber distribution case is given in Table 5.

The optimal fiber distribution of the first and second ply layers follows a parabolic type distribution for the AR of 1.0 and 1.3. For the AR of 2.0, the first ply is almost 60% VF and the second ply is 20% VF. However, the plies of AR 4.0 follow corrugated type distributions with 60% VF for the first ply and 20% VF for the second ply. Table 4 shows that the parabolic and corrugated type distributions have better flexibility and bending stiffness compared to the uniform fiber distribution. The FR ratio for the optimal results show an increase of 31–47% from the uniform fiber distribution as given in Table 5. Also, the FR for the optimal results of case I show an increase of 27–40% and the 60/20 VF case shows an increase of 29% from the uniform fiber distribution.

In addition to the above results, the FR of the laminate with a uniform distribution of VF of fibers varying from 20% to 60% is shown in Fig. 11. The results show that the FR increases with the VF of fibers in a non-linear manner and converges for the VF above 60%. This can be understood as the fibers dominate the laminate for the VF above 60%. However, the FR of the laminate with a uniform VF of 60% is less than the FR of the optimal distributions whose average VF is 40%. These results clearly show that the variable fiber volume distributions enhance the characteristics desirable for morphing skin applications.

4. Conclusion

An optimization is performed to enhance the in-plane flexibility and bending stiffness of morphing wing skins modeled as composite plates. Initially, the optimal fiber and elastomer materials for a highly flexible fiber reinforced elastomer laminate are studied. In the next stage, the effects of boundary conditions and aspect ratio on the out-of-plane deflection of a composite laminate are studied. Finally, an optimization is performed to minimize the in-plane stiffness and maximize the bending stiffness, simultaneously, by spatially varying the fiber distribution of a laminate. The following conclusions are drawn from this study:

1. The longitudinal Young's modulus and major Poisson's ratio of FRE lamina show considerable variation for the various fiber and elastomer properties considered. The lateral and shear modulus are of the order 10^{-3} less than longitudinal modulus. The minor Poisson's ratio is of the order of 10^{-3} for all of the fiber and elastomer combinations because of the highly orthotropic nature of the FRE lamina. The preliminary results show that most of the elastomers satisfies the stiffness and Poisson's ratio requirements of the morphing skins. However, the non-linear stress–strain behavior, the elastic recovery and the thermal resistant property of elastomers are major parameters in designing the FRE lamina for morphing skins and have to be investigated.
2. The aspect ratio and boundary conditions have a considerable influence on the out-of-plane deflection of plate. Therefore, the optimal distribution of volume fraction of fiber changes with the aspect ratio of the plate.
3. The optimization performed to minimize the out-of-plane deflection shows that the parabolic type fiber distributions increase the bending stiffness. The optimal fiber distribution minimizes the out-of-plane deflection by 25–30% compared to the uniform fiber distribution.
4. The optimization performed to increase the flexibility ratio of the laminate has shown that the non-uniform distribution of fibers increases the flexibility ratio by almost 30–47% when compared to a uniform distribution of fibers. The flexibility

ratio of optimal fiber distributions with an average volume fraction of 40% is higher than the uniform fiber distribution with a volume fraction of 60%.

These results clearly show that the variable fiber distribution plays a major role in enhancing the characteristics of composite laminates desirable for morphing skins.

Acknowledgments

The authors acknowledge the support of the European Research Council through Project 247045 entitled "Optimization of Multi-scale Structures with Applications to Morphing Aircraft".

E.I. Saavedra Flores gratefully acknowledges the support of the Department of Civil Engineering, University of Santiago, Chile.

References

[1] Thill C, Etches J, Bond I, Potter K, Weaver P. Morphing skins. Aeronaut J 2008;112(1129):117–39.
[2] Olympio KR, Gandhi F. Zero Poisson's ratio cellular honeycombs for flex skins undergoing one-dimensional morphing. J Intell Mater Syst Struct 2010;21(17):1737–53.
[3] Peel LD, Mejia J, Narvaez B, Thompson K, Lingala M. Development of a simple morphing wing using elastomeric composites as skins and actuators. J Mech Des 2009;131(9):091003.
[4] Murray G, Gandhi F, Bakis C. Flexible matrix composite skins for one-dimensional wing morphing. J Intell Mater Syst Struct 2010;21(17):1771–81.
[5] Bubert EA. Highly extensible skin for a variable wing-span morphing aircraft utilizing pneumatic artificial muscle actuation, MS thesis. College Park: University of Maryland; 2009.
[6] Kikuta MT. Mechanical properties of candidate materials for morphing wings, MS thesis. Blacksburg (Virginia): Virginia Polytechnic Institute and State University; 2009.
[7] Gurdal Z, Tatting B, Wu C. Variable stiffness composite panels: effects of stiffness variation on the in-plane and buckling response. Composites Part A 2008;39(5):911–22.
[8] Leissa A, Martin A. Vibration and buckling of rectangular composite plates with variable fiber spacing. Compos Struct 1990;14(4):339–57.
[9] Benatta M, Mechab I, Tounsi A, Bedia EA. Static analysis of functionally graded short beams including warping and shear deformation effects. Comput Mater Sci 2008;44(2):765–73.
[10] Kuo S-Y, Shiau L-C. Buckling and vibration of composite laminated plates with variable fiber spacing. Compos Struct 2009;90(2):196–200.
[11] Kuo S-Y. Flutter of rectangular composite plates with variable fiber pacing. Compos Struct 2011;93(10):2533–40.
[12] Wolfe WE, Butalia TS. A strain–energy based failure criterion for non-linear analysis of composite laminates subjected to biaxial loading. Compos Sci Technol 1998;58(7):1107–24.
[13] Ochoa OO, Reddy JN. Finite element analysis of composite laminates. Dordrecht: Kluwer Academic Publishers; 1992.
[14] Peel LD. Exploration of high and negative Poisson's ratio elastomer–matrix laminates. Phys Status Solidi (b) 2007;244(3):988–1003. doi:10.1002/pssb.200572717.
[15] ANSYS. Release 11.0 documentation for ANSYS. Southpointe (Canonsburg, PA 15317): ANSYS, Inc.; 2007.
[16] Giusti SM, Blanco PJ, de Souza Neto EA, Feijóo RA. An assessment of the Gurson yield criterion by a computational multi-scale approach. Eng Comput 2009;26(3):281–301.
[17] Saavedra Flores EI, de Souza Neto EA. Remarks on symmetry conditions in computational homogenisation problems. Eng Comput 2010;27(4):551–75.
[18] Bowen CR, Dent AC, Nelson LJ, Stevens R, Cain MG, Stewart M. Failure and volume fraction dependent mechanical properties of composite sensors and actuators. Proc IMechE Part C: J Mech Eng Sci 2006;220(C11):1655–64.
[19] Murugan M, Suresh S, Ganguli R, Mani V. Target vector optimization of composite box beam using real-coded genetic algorithm: a decomposition approach. Struct Multidisc Optim 2007;33:131–46.